Color measurement of the animal integument predicts the content of specific melanin forms

Ismael Galván[1,*] and Kazumasa Wakamatsu[2]

[1]Department of Evolutionary Ecology, Doñana Biological Station - CSIC, 41092 Sevilla, Spain. [2]Department of Chemistry, Fujita Health University School of Health Sciences, Toyoake, Aichi 470-1192, Japan.

*Author for correspondence (galvan@ebd.csic.es)

Abstract

The appearance of animals largely depends on melanins present in their integument. However, it is unclear how different melanin forms create different animal color phenotypes. We used reflectance spectrophotometry to measure the color expression of feathers and hairs of 59 species of birds and 12 species of mammals, comprising a significant part of the palette of melanin-based colors, and analyzed for the first time the detailed chemical composition of melanins on the same samples by HPLC. We quantified color variation by means of the slope of percent reflectance regressed against wavelength, as this was the best predictor of a human categorization of color phenotypes, increasing with the following scale: black, grey, dark brown, dark orange, light brown and light orange. Color slope variation was explained by levels of the 5,6-dihydroxyindole-2-carboxylic acid (DHICA) unit of eumelanin and the benzothiazole moiety of pheomelanin in feathers and hairs, but not by levels of the 5,6-dihydroxyindole (DHI) unit of eumelanin nor the benzothiazine moiety of pheomelanin. DHICA-eumelanin and benzothiazole-pheomelanin components explained color expression in opposite ways, decreasing and increasing, respectively, with color slope. Color slope, and also color categorization as perceived by humans, can therefore be used to infer the melanin chemical composition of feathers and hairs. Given that cytotoxic reactive oxygen species (ROS) are more abundantly formed during the synthesis of DHI than during the synthesis of DHICA in eumelanins, and in pheomelanins with higher benzothiazine/benzothiazole ratios, melanin-based colors interestingly reflect the content of the less pro-oxidant melanin forms.

Introduction

The visual appearance of most organisms depends to some extent on the presence of melanins in their integument. Melanins are thus the most extended biological pigments, and certainly the most abundant in higher vertebrates[1]. Melanins are divided into eumelanins, polymers composed of indole units, and pheomelanins, composed of sulphur-containing heterocycles[2]. The chemical heterogeneity of melanins gives them different optical properties in the visible spectral range, hence providing a diversity of colors to skin and its associated structures such as scales, feathers and hairs when melanosomes (i.e., specialized organelles of melanocytes where melanin synthesis takes place) are transferred to surrounding epidermal keratinocytes[3].

It is known that eumelanins are darker than pheomelanins, the former conferring black, brown and grey colors and the latter conferring yellowish and reddish colors[4]. However, the entire diversity of color phenotypes that can be generated by melanins is still unknown. Previous studies have investigated how different color parameters of the animal integument predict the total content of eumelanin and pheomelanin[5], but melanin diversity is greater than just eumelanin and pheomelanin[6]. By using synchrotron-based photoionization mass spectrometry, Liu *et al.*[7] associated different structural components of eumelanin and pheomelanin to different animal colors, but the lack of specific markers of those components (i.e., standards) and quantitative descriptions of colors make that additional analyses are needed to firmly infer an association between melanin chemistry and color phenotype. This will have broad implications, as a great interest exists in deciphering the color phenotype of extinct animals based on information on fossilized melanins[8] and in finding potential trade-offs between physiological costs and benefits of producing different melanin structural units[6].

Therefore, here we aimed at analyzing the expression of colors in natural melanins covering the entire palette of melanin-based traits in birds and mammals, and investigating

78 how the different components of eumelanin and pheomelanin polymers explain that

79 variability.

80   Melanocytes usually produce both eumelanins and pheomelanins from the common

81 precursor dopaquinone that is formed by the oxidation of L-tyrosine. Eumelanin is formed

82 when sulfhydryl compounds are absent or below certain levels in melanocytes, while

83 pheomelanin is formed when sulfhydryls are above a threshold level and get incorporated

84 to the process[2]. The indole units of eumelanins, which are composed of 5,6-

85 dihydroxyindole (DHI) and 5,6-dihydroxyindole-2-carboxylic acid (DHICA) moieties, result

86 from the decarboxylative or nondecarboxylative rearrangement of dopachrome, a product

87 derived from dopaquinone cyclization[9]. Pheomelanin units, by contrast, are composed of

88 benzothiazine and benzothiazole moieties[10]. High-performance liquid chromatography

89 (HPLC) allows the detection of specific degradation products of melanins that are specific

90 to the different structural units of eumelanins and pheomelanins. In particular, pyrrole-

91 2,3,5-tricarboxylic acid (PTCA) and pyrrole-2,3-dicarboxylic acid (PDCA), which are

92 specific markers of DHICA and DHI eumelanin units, respectively, and 4-amino-3-

93 hydroxyphenylalanine (4-AHP) and thiazole-2,4,5-tricarboxylic acid (TTCA), which are

94 specific of benzothiazine and benzothiazole pheomelanin moieties, respectively[11,12].

95   We used HPLC to measure levels of PTCA, PDCA, 4-AHP and TTCA in feathers of

96 59 species of birds and hairs of 12 species of mammals, comprising a comprehensive

97 diversity of colors that natural melanins can generate (Fig. 1). For this, we obtained 1-2

98 feathers from 1-2 bird specimens deposited in museum collections for each species,

99 complemented by samples obtained from wild populations (Table S1). Similarly, we

100 obtained 10-15 hairs from 1-2 mammal specimens deposited in museum collections for

101 each species (Table S1). The species were chosen on the basis of homogeneity in the

102 color patches that were analyzed, i.e. avoiding complex plumage or pelage patterns

103   consisting in differently perceived color hues. We avoided iridescent colorations, as these

104   are generated by melanosome morphology and not by melanin chemistry[13].

105

106   **Methods**

107   **HPLC analyses**

108   Feather and hair samples were first homogenized with Ten-Broeck glass homogenizer at a

109   concentration of 10 mg/ml water (removing barbs and rachis parts not corresponding to

110   the target color patch in the case of feathers), and then using alkaline H_2O_2 oxidation of

111   eumelanin and pheomelanin to measure PTCA, PDCA and TTCA levels[12] and reductive

112   hydrolysis of pheomelanin with hydriodic acid (HI) to measure 4-AHP levels[11].

113   For 4-AHP analyses, 100 μl of sample homogenate was taken in a 10 ml screw-

114   capped conical test tube, to which 20 μl 50% H_3PO_2 and 500 μl 57% HI were added. The

115   tube was heated at 130 °C for 20 h, after which the mixture was cooled. An aliquot (100 μl)

116   of each hydrolysate was transferred to a test tube and evaporated to dryness using a

117   vacuum pump connected to a dry ice-cooled vacuum trap and two filter flasks containing

118   NaOH pellets. The residue was dissolved in 200 μl 0.1 M HCl. An aliquot (10-20 μl) of

119   each solution was analysed on the HPLC system (JASCO 880-PU pump, JASCO

120   Catecholpak C18 column and EICOM ECD-300 electrochemical detector; Eicom, Kyoto,

121   Japan). A standard solution (10-20 μl) containing 500 ng each of 4-AHP (synthesized by

122   K. W.) and 3-AHP (3-amino-4-hydroxyphenylalanine; 3-aminotyrosine from Sigma) in 1 mL

123   0.1 M HCl was injected every 10 samples (Fig. 2).

124   For PTCA, PDCA and TTCA analyses, 100 μl of sample homogenate was taken in

125   a 10 ml screw-capped conical test tube, to which 375 μl 1 M K_2CO_3 and 25 μl 30% H_2O_2

126   (final concentration: 1.5%) were added. The mixture was mixed vigorously at 25 ± 1 °C for

127   20 h. The residual H_2O_2 was decomposed by adding 50 μl 10% Na_2SO_3 and the mixture

128   was then acidified with 140 μl 6 M HCl. After vortex-mixing, the reaction mixture was

129   centrifuged at 4000 g for 1 min, and an aliquot (80 μl) of the supernatant was directly

130   injected into the HPLC system (JASCO 880-PU pump, Shiseido Capcell Pak MG C18

131   column and JASCO UV detector; Shiseido Co., Ltd., Tokyo, Japan). A standard solution

132   (80 μl) containing 1 μg each of PTCA, PDCA, TTCA and TDCA (thiazole-2,3-dicarboxylic

133   acid) in 1 mL water was injected every 10 samples. All these standards were synthesized

134   by K. W. (Fig. 2).

135   Resulted values were multiplied by a conversion factor (PTCA: 25, PDCA: 50, 4-

136   AHP: 9, TTCA: 34) to obtain absolute amounts of markers per mg of feather or hair. HPLC

137   analyses were conducted blindly from results of spectrophotometric analyses (see below).

138

139   **Spectrophotometric analyses**

140   Before conducting HPLC analyses, we measured the color expression of feathers and

141   hairs by reflectance spectrophotometry. Thus, these analyses were conducted without any

142   information on the melanin contents of samples. We used an Ocean Optics Jaz

143   spectrophotometer (range 220-1000 nm) with ultraviolet (deuterium) and visible (tungsten-

144   halogen) lamps and a bifurcated 400 micrometer fiber optic probe. The fiber optic probe

145   both provided illumination and obtained light reflected from the sample, with a reading

146   area of ca. 1 mm^2. Feathers were mounted on a light absorbing foil sheet (Metal Velvet

147   coating, Edmund Optics, Barrington, NJ) to avoid any background reflectance.

148   Measurements were taken at a 90º angle to the sample. All measurements were relative to

149   a diffuse reflectance standard tablet (WS-1, Ocean Optics, Dunedin, FL), and reference

150   measurements were frequently made. An average spectrum of five-six readings on

151   different points of the target color patches in feathers or hairs was obtained for each bird,

152   removing the probe after each measurement. The analyses were made on individual

153   feathers separately, and mean spectra were then calculated. Given the small size of hairs,

154   measurements were not taken on individual hairs but on the groups of 10-15 hairs from

155   each specimen. Reflectance curves were determined by calculating the median of the

156   percent reflectance in 10 nm intervals. As we were interested in investigating the diversity

157   of melanin-based colors as perceived by humans, we only considered the visible spectral

158   range (400-700 nm) in the analyses.

159   Spectral data were summarized as a measure of total brightness, as this is currently

160   considered the best predictor of total levels of melanins in feathers, with lower values (i.e.,

161   darker colors) denoting higher melanin contents[5]. Brightness was defined as the summed

162   reflectance across the entire spectral range. Additionally, as the reflectance of melanins

163   steadily increases from 300 to 700 nm and shows no spectral peaks[14], variation in the

164   perceived color generated by melanins may be given to a large extent by variation in the

165   slope of the reflectance curves (Fig. 3). We therefore calculated the slope of reflectance

166   regressed against wavelength in the 400-700 nm range (Fig. 3) and used it as an

167   additional descriptive measurement of melanin-based color expression.

168

169   **Statistical analyses**

170   The same feathers/hairs that were analyzed by reflectance spectrophotometry were then

171   measured by HPLC as described above, with some exceptions for which we could only

172   analyze samples from different specimens with each technique (Table S1). We thus

173   investigated the differential contribution of PTCA, PDCA, 4-AHP and TTCA levels

174   (predictor variables) to explain variability in color expression (brightness or slope;

175   response variables). We used partial least squares regression (PLSR) analyses[15], as this

176   is an appropiate statistical technique to analyzing the predictive capacity of melanin

177   markers, which use to be highly intercorrelated[16]. Indeed, in this case the degree of

178   correlation between these variables was high (PTCA-PDCA: $r = 0.44$, $P < 0.0001$; PTCA-

179   4-AHP: $r = -0.31$, $P = 0.008$; PTCA-TTCA: $r = -0.19$, $P = 0.102$; PDCA-4-AHP: $r = 0.10$, $P = $

180   0.414; PDCA-TTCA: $r = 0.25$, $P = 0.030$; 4-AHP-TTCA: $r = 0.73$, $P < 0.0001$; $n = 74$).

181 Melanin markers were $\log_{10}$-transformed prior to analyses to achieve normality

182 assumptions.

183 The significance of the extracted PLSR components was determined with two

184 criteria. First, a cross-validation test of the parameter Q^2 was carried out to determine if a

185 component was significant. Then, we tested the significance of the correlation coefficient

186 of the relationship between PLSR scores for the response variable and PLSR component

187 scores, thus determining if the amount of variance explained in the response variable was

188 significant. We also tested the statistical significance of the regression coefficients of the

189 predictors in the PLSR analyses, to determine the degree of correlation between the

190 response variable and these predictors. The latter test was made by bootstrapping using

191 100 replications. All PLSR analyses were made with the software TANAGRA 1.4[17].

192 As our interest was to investigate the diversity of melanin-based colors as perceived

193 by humans, we assigned the studied species to one of six color categories (on the basis of

194 perception of the museum specimens used in the study) to determine which reflectance

195 measurement (brightness or slope) best predicted the human perception of color. We

196 assigned a value to these categories that increased with decreasing perceived darkness

197 (i.e., increased from black to orange). Although this constitutes a subjective categorization

198 of color, it was simply made as a convenient way to relate quantitative color

199 measurements (brightness and slope) to the human perception of melanin-based color

200 variation. Thus, color categories and their corresponding values were: black (1), grey (2),

201 dark brown (3), dark orange (4), light brown (5) and light orange (6) (Fig. 1). We therefore

202 regressed brightness and slope against this scale, and found that color category

203 significantly predicted both brightness and slope, although the correlation coefficient was

204 higher for slope (r = 0.69, n = 74, P < 0.0001; slope = -0.0071 + 0.0129 x color category)

205 than for brightness (r = 0.47, n = 74, P < 0.0001; Fig. 4). This indicates that our

206 measurement of slope reliably explains the perceived variation in melanin-based color

207 phenotypes, explaining a higher proportion of that variation than brightness. Thus, we

208 used the slope as a response variable in the PLSR analyses to investigate the association

209 between melanin chemistry and color expression. It must be noted that color

210 categorization is a simple measurement just aiming at testing if melanin composition of

211 feathers and hairs correlates with the general variation in color that is perceived by

212 humans. Slope is still highly correlated with color category even if different orders of

213 categories, for example assigning a value of 4 to grey colors as these may sometimes be

214 perceived as darker than dark brown and dark orange colors, are considered ($r = 0.50$, $P <$

215 0.0001).

216

217 **Results**

218 The PLSR analysis generated one significant component that explained 44 % of variance

219 in color slope, which was significantly correlated with this component ($r = 0.73$, $n = 74$, $P <$

220 0.0001; Fig. 5). This component was negatively related to PTCA levels (predictor weight =

221 -0.70) and to PDCA levels (predictor weight = -0.28), and positively related to 4-AHP levels

222 (predictor weight = 0.49) and to TTCA levels (predictor weight = 0.44). As the square of

223 predictor weights indicates the proportion of variance explained by the PLSR component

224 (i.e., 44 %) that is explained by each predictor variable[15], it follows that PTCA levels

225 accounted for most variation in color slope, explaining 22 % of variance in this variable.

226 Bootstrapping analyses showed that the regression coefficients were significant in the

227 case of PTCA (-0.030, $P < 0.005$) and TTCA (0.012, $P < 0.05$), but not in the case of

228 PDCA (-0.006, $0.2 < P < 0.3$) and 4-AHP (0.004, $0.4 < P < 0.5$). Thus, variation in the

229 perceived variation in melanin-based colors reflects variation in PTCA and TTCA levels,

230 the contribution of PDCA and 4-AHP being non-significant in explaining this variation (Fig.

231 5).

232   To corroborate the results of the PLSR model and to obtain a simple predictive

233   equation, we conducted a general linear model (GLM) regressing color slope against the

234   only two significant predictors that resulted from the PLSR model (i.e., PTCA and TTCA).

235   PTCA and TTCA values (as ng/mg) were added to the model without any transformations,

236   neither logarithmic nor applying conversion factors. The GLM model explained a

237   significant proportion of variance in color slope (31 %, $F_{2,73}$, $P < 0.0001$), and the resulting

238   equation was: slope = 0.0409 + (-3.1347 x 10^{-5} x PTCA) + (1.4753 x 10^{-5} x TTCA). We

239   used this equation to test the capacity of PTCA and TTCA to predict the color slope of

240   animals in different datasets from other studies. We then used the equation relating color

241   slope to color category (see Methods above) to predict the color phenotype. In particular,

242   we used available data of melanin contents in different color forms of the hair of alpacas

243   *Vicugna pacos*[18] and house mice *Mus musculus* and humans[12] (Table 1). Assuming that

244   predicted color categories around zero correspond to the lowest color category considered

245   here (i.e., 1 = black), and that rose grey forms correspond to brown colors and fawn forms

246   correspond to orange colors in alpaca[18], our data predicted the color of 12 out of 20 cases

247   (i.e., 60 %; Table 1). This, however, must be taken with caution as color nomenclature in

248   alpacas is not standardised and often confusing[18].

249

Discussion

251   Our findings indicate that color slope, measured as percent reflectance regressed against

252   wavelength, can be used to predict the melanin chemical composition of feathers and

253   hairs. As slope was strongly correlated with a scale of color expression variation as

254   perceived by humans, these color categories (black, grey, dark brown, dark orange, light

255   brown and light orange) are equally useful to determine melanin composition. However,

256   slope is a continuous variable, meaning that it can quantify color variation within a single

257   color category in the scale of human perception. Therefore, slope is the most useful

258 measurement to determine the melanin composition of feathers and hairs. However, our

259 PLSR model explained 44 % of variance in color slope, thus leaving ca. 60 % of variance

260 unexplained. This means that, although our study shows that the resulting color phenotype

261 is clearly associated with the concentration of certain melanin forms, there may be other

262 factors that are more relevant for explaining the expression of color than melanin

263 concentration. Future studies should explore these factors.

264 Our results show that the color phenotype of birds and mammals reflects the

265 content of the carboxylated (DHICA) unit of eumelanin and the content of the

266 benzothiazole moiety of pheomelanin. No color phenotype is only generated by DHICA or

267 benzothiazoles. Rather, color variation reflects different combinations of the two

268 components: black colors contain the highest contents of DHICA and the lowest contents

269 of benzothiazoles, while the opposite applies to light orange colors. These results differ

270 from those previously found by Liu *et al.*[7]. They concluded that black color is generated by

271 the two units of eumelanin (DHI and DHICA) with no contribution of pheomelanin, that

272 brown color is mainly generated by pheomelanin with contribution of both benzothiazines

273 and benzothiazoles and that grey color is mainly generated by pheomelanins, although

274 standards of melanin units were not used in these analyses.

275 This study represents the first detailed chemical analysis of melanins in a wide

276 range of melanin-based color phenotypes in animals. Our findings have implications to

277 understand the evolution of animal coloration. During the final stages of eumelanogenesis,

278 significant amounts of cytotoxic species, including reactive oxygen species (ROS) such as

279 superoxide and hydrogen peroxide, are formed in melanocytes. The amount of ROS

280 generated is much greater during the formation of DHI than during the formation of DHICA,

281 as supported by a lower survival of melanocytes with no activity of the enzymes Tyrp1 and

282 Tyrp2, which are involved in the DHICA route[19-21]. This is because DHICA melanin exhibits

283 potent hydroxyl radical-scavenging properties in the Fenton reaction while DHI melanin

284   does not[21], and because the delocalized π-electron systems of the DHI polymer makes it

285   generates a broader variety of free radical species than DHICA melanin[22]. As selection is

286   blind to genes and only acts on phenotypes, it is likely that individuals with color

287   phenotypes denoting high carboxylated eumelanin contents are selected because of these

288   protective benefits independently of other benefits that uncarboxylated eumelanin may

289   confer (e.g., a higher protection against UV radiation)[6]. On the other hand, color

290   phenotypes denoting pheomelanins with high relative benzothiazole contents would be

291   selected for similar reasons to those suggested above for eumelanin, as, once formed,

292   such pheomelanins produce less ROS under exposure to energetic radiation (such as UV

293   or ionizing radiation) than pheomelanins with higher benzothiazine contents[10,23-26].

294   Interestingly, then, melanin-based color phenotypes reflect the content of the less

295   pro-oxidant melanin forms (i.e., DHICA-eumelanin and benzothiazole-pheomelanin), so

296   selection may act on these phenotypes because of the same potential adaptive benefits

297   related to the avoidance of cytotoxicity during or after melanogenesis. Whether selection

298   pressure correlates positively or negatively with the color phenotype gradient (i.e., vertical

299   axis in Fig. 5) will probably depend on the differential benefits that eumelanin[27,28] and

300   pheomelanin[14,29] confer to individuals. These predictions for selective effects on melanin-

301   based coloration should be valid for comparisons within color phenotypes (e.g., individuals

302   with more intense black or grey coloration vs others with less intense coloration) as well as

303   comparisons between color phenotypes. They should also be useful to identify individuals

304   or species particularly susceptible to the effects of environmental oxidative stress[24], a

305   possibility that should be explored in humans regarding hair and skin coloration.

306   Lastly, given the current interest in determining the chemical composition of

307   fossilized melanin granules to infer the color of extinct animals[8,30,31], our findings represent

308   a key tool to elucidate the color corresponding to fossil specimens for which melanin

309   composition can be established. The morphology of fossilized melanin granules has been

310   used in some studies as a predictor of feather color in extinct birds, in all cases

311   considering that granule morphology is related to melanin chemistry and then to the color

312   being expressed[32,33]. Our study provides a direct association between melanin chemistry

313   and color with a proven predictive capacity of the melanin-based coloration of animals. It

314   must be considered, however, that our data only predicted 60 % of cases of alpaca,

315   mouse and human hair color for which PTCA and TTCA values had been reported in other

316   studies. Further work is necessary to get a proper understanding of all factors contributing

317   to the expression of melanin-based coloration, including sources of variation not related to

318   the concentration of different melanin forms. Only this comprehensive understanding will

319   allow to make precise predictions of the color of extinct and extant animals.

320

333

References

335   1 F. Solano, *New J. Sci.*, 2014, **2014**, 498276.

336   2 S. Ito and K. Wakamatsu, *Photochem. Photobiol.*, 2008, **84**, 582-592.

337   3 M. d'Ischia, K. Wakamatsu, F. Cicoira, E. Di Mauro, J. C. García-Borrón, S. Commo, I.

338   Galván, G. Ghanem, K. Kenzo, P. Meredith, A. Pezzella, C. Santato, T. Sarna, J. D.

339   Simon, L. Zecca, F. A. Zucca, A. Napolitano and S. Ito, *Pigment Cell Melanoma*

340   *Res.*, 2015, **28**, 520-544.

341   4 I. Galván, J. Erritzøe, K. Wakamatsu and A. P. Møller, *Comp. Biochem. Physiol. A*,

342   2012, **162**, 259-264.

343   5 K. J. McGraw, R. J. Safran and K. Wakamatsu, *Funct. Ecol.*, 2005, **19**, 816-821.

344   6 I. Galván, and F. Solano, *Physiol. Biochem. Zool.*, 2015, **88**, 352-355.

345   7 S. Y. Liu, M. D. Shawkey, D. Parkinson, P. Tyler, T. P. Troy and M. Ahmed, *RSC Adv.*,

346   2014, **4**, 40396-40399.

347   8 J. Vinther, *BioEssays*, 2015, **37**, 643-656.

348   9 M. d'Ischia, A. Napolitano, A. Pezzella, P. Meredith and T. Sarna, *Angew. Chem. Int.*

349   *Ed.*, 2009, **48**, 3914-3921.

350   10 K. Wakamatsu, K. Ohtara and S. Ito, *Pigment Cell Melanoma Res.*, 2009, **22**, 474-486.

351   11 K. Wakamatsu, S. Ito and J. L. Rees, *Pigment Cell Res.*, 2002, **15**, 225-232.

352   12 S. Ito, Y. Nakanishi, R. K. Valenzuela, M. H. Brilliant, L. Kolbe and K. Wakamatsu,

353   *Pigment Cell & Melanoma Research*, 2011, **24**, 605-613.

354   13 C. M. Eliason, P. P. Bitton, and M. D. Shawkey, *Proc. R. Soc. B*, 2013, **280**, 20131505.

355   14 I. Galván, and A. P. Møller, *Physiol. Biochem. Zool.*, 2013, **86**, 184-192.

356   15 L. M. Carrascal, I. Galván and O. Gordo, *Oikos*, 2009, **118**, 681-690.

357   16 I. Galván, A. Jorge, K. Ito, K. Tabuchi, F. Solano and K. Wakamatsu, *Pigment Cell*

358   *Melanoma Res.*, 2013, **26**, 917-923.

359   17 R. Rakotomalala, *Proceedings of EGC'2005, RNTI-E-3*, 2005, **2**, 697-702 (in French).

360   18 R. Cransberg, K. Wakamatsu, and K. Munyard, *Small Ruminant Res.*, 2013, **114**, 240-

361   246.

362   19 V. J. Hearing, *Am. J. Hum. Genet.*, 1993, **52**, 1-7.

363   20 K. Urabe, P. Aroca, K. Tsukamoto, D. Mascagna, A. Palumbo, G. Prota and V. J.
364   Hearing, *Biochim. Biophys. Acta*, 1994, **1221**, 272-278.

365   21 S. Jiang, X. M. Liu, X. Dai, Q. Zhou, T. C. Lei, F. Beermann, K. Wakamatsu and S. Z.
366   Xu, *Free Radic. Biol. Med.*, 2010, **48**, 1144-1151.

367   22 R. Micillo, L. Panzella, K. Koike, G. Monfrecola, A. Napolitano and M. d'Ischia, *Int. J.*
368   *Mol. Sci.*, 2016, **17**, 746.

369   23 K. Wakamatsu, Y. Nakanishi, N. Miyazaki, L. Kolbe and S. Ito, *Pigment Cell Melanoma*
370   *Res.*, 2012, **25**, 434-445.

371   24 I. Galván, A. Bonisoli-Alquati, S. Jenkinson, G. Ghanem, K. Wakamatsu, T. A.
372   Mousseau and A. P. Møller, *Funct. Ecol.*, 2014, **28**, 1387-1403.

373   25 A. Napolitano, L. Panzella, G. Monfrecola and M. d'Ischia, *Pigment Cell Melanoma*
374   *Res.*, 2014, **27**, 721-733.

375   26 L. Panzella, L. Leone, G. Greco, G. Vitiello, G. D'Errico, A. Napolitano and M. d'Ischia,
376   *Pigment Cell Melanoma Res.*, 2014, **27**, 244-252.

377   27 G. R. Bortolotti, in *Bird Coloration, Volume II: Function and Evolution*, ed G. E. Hill and
378   K. J. McGraw, Harvard University Press, Cambridge, 2006, pp. 3-35.

379   28 M. Brenner and V. J. Hearing, *Photochem. Photobiol.*, 2008, **84**, 539-549.

380   29 H. E. Hoekstra, R. J. Hirschmann, R. A. Bundey, P. A. Insel and J. P. Crossland,
381   *Science*, 2006, **313**, 101-104.

382   30 J. A. Clarke, D. T. Ksepka, R. Salas-Gismondi, A. J. Altamirano, M. D. Shawkey, L.
383   D'Alba J. Vinther, T. J. DeVries and P. Baby, *Science*, 2010, **330**, 954-957.

384   31 F. Zhang, S. L. Kearns, P. J. Orr, M. J. Benton, Z. Zhou, D. Johnson, X. Xu and X.
385   Wang, *Nature*, 2010, **463**, 1075-1078.

386   32 R.M. Carney, J. Vinther, M. D. Shawkey, L. D'Alba and J. Ackermann, *Nat. Commu.*,
387   2012, **3**, 637.

388   33 Q. Li, J. A. Clarke, K. Q. Gao, C. F. Zhou, Q. Meng, D. Li, L. D'Alba and M. D.

389   Shawkey, *Nature*, 2014, **507**, 350-353.

390   34 M. J. Crawley, *GLIM for Ecologists*. Blackwell Science, Oxford, 1993.

391

392

393

394

395

396

397

398

399

400

401

402

403

404

405

406

407

408

409

410

411

412

413

Table 1. PTCA and TTCA levels in the hair of different color forms of alpacas, mice and humans from previously published sources[12,18], and color slope and category predicted from data in this study. Descriptions of hair color correspond to those provided by the authors of the published sources.

Species	Hair color	PTCA (ng/mg)	TTCA (ng/mg)	Predicted slope	Predicted color category	Congruence
Alpaca	Black	2145	200	-0.023	-1.26	Yes
	Black brown	1526	329	-0.002	0.39	Yes
	Grey	1041	108	0.010	1.31	No
	Silver grey	988	194	0.013	1.54	Yes
	Rose grey	419	490	0.035	3.26	Yes
	Red/brown	179	1372	0.056	4.85	Yes
	Dark brown	130	764	0.048	4.28	No
	Chestnut	99.2	1084	0.054	4.72	Yes
	Brown	43.2	378	0.045	4.05	No
	Light brown	25.3	151	0.042	3.83	No
	Fawn	14.6	70.4	0.041	3.77	Yes
	Pink-skin fawn	13.1	143	0.043	3.85	Yes
	Dark-skin fawn	7.6	98.3	0.042	3.81	Yes
	White	4.1	7.8	0.041	3.72	No
	Light fawn	2.4	21.3	0.041	3.74	Yes
Mouse	Black (a/a)	2000	97	-0.020	-1.03	Yes
	Yellow (e/e)	121	243	0.041	3.70	No
Human	Black	340	98	0.032	3.01	No
	Blonde	39	38	0.040	3.67	No
	Red	62	89	0.040	3.67	Yes

429 **Legends to figures:**

430

431 **Fig. 1.** Images of species included in the study, showing the color patches that were

432 analyzed. The names of the species are provided in Table S1. Note that some species

433 were included in two color categories because two different color patches were analyzed

434 in the same specimens (see Table S1). These images are only used to show the

435 appearance of the species included the study, not to determine color categories. The

436 photographs, with the exception of #53 which belongs to one of the authors of the study (I.

437 G.), are covered by a CC BY license (https://creativecommons.org/licenses/by/2.0/;

438 photographs #1-6, 10, 12, 14, 15, 17, 19, 20, 22-24, 30, 32-34, 42, 44, 46, 47, 54, 55, 57,

439 58, 60 and 64-70) or by a CC BY-SA license (https://creativecommons.org/licenses/by-

440 sa/2.0/; photographs #7-9, 11, 13, 16, 18, 21, 25-29, 31, 35-41, 43, 45, 48-52, 56, 59 and

441 61-63).

442 Photograph credits and links: #1 (Tony Smith; https://flic.kr/p/fq4NP7), #2 (procristination;

443 https://flic.kr/p/5cEteB), #3 (James St. John; https://flic.kr/p/dCphEp), #4 (Peter von Bagh;

444 https://flic.kr/p/C7A9gd), #5 (Stefan Berndtsson; https://flic.kr/p/egDf2V), #6 (Ekaterina

445 Chernetsova (Papchinskaya); https://flic.kr/p/mVCZEz), #7 (Dornenwolf;

446 https://flic.kr/p/kY9J7W), #8 (John Haslam; https://flic.kr/p/KnYBS), #9 (Bernard DUPONT;

447 https://flic.kr/p/d47kkd), #10 (big-ashb; https://flic.kr/p/r2bEQV), #11 (Francesco Veronesi;

448 https://flic.kr/p/vynehC), #12 (Hans G Bäckman; https://flic.kr/p/jqd9CJ), #13 (Larry Miller;

449 https://flic.kr/p/eKGHsS), #14 (Joe McKenna; https://flic.kr/p/bWjLLw), #15 (Smabs

450 Sputzer; https://flic.kr/p/fGaoLk), #16 (harum.koh; https://flic.kr/p/qAAgEe), #17 (Vibhu

451 Prasad; https://flic.kr/p/9CeLfU), #18 (Bernard DUPONT; https://flic.kr/p/srHCWr), #19

452 (nociveglia; https://flic.kr/p/d9vtmu), #20 (Ingrid Taylar; https://flic.kr/p/eZhjvt), #21

453 (sébastien bertru; https://flic.kr/p/ePV5UK), #22 (Michele Lamberti;

454 https://flic.kr/p/hg5mFP), #23 (Michele Lamberti; https://flic.kr/p/ea4doW), #24 (robin_24;

455   https://flic.kr/p/93q8Nc), #25 (Sciadopitys; https://flic.kr/p/aYXDqz), #26 (Juan Emilio;

456   https://flic.kr/p/bHtiui), #27 (Susanne Nilsson; https://flic.kr/p/DthK7w), #28 (Bernard Stam;

457   https://flic.kr/p/dFn5Up), #29 (Ferran Pestaña; https://flic.kr/p/8RKUWq), #30 (Stefan

458   Berndtsson; https://flic.kr/p/f3zxHq), #31 (rjime31; https://flic.kr/p/55skE2), #32 (Peter

459   Trimming; https://flic.kr/p/a2jNtS), #33 (Peter Trimming; https://flic.kr/p/cbndLG), #34 (Noel

460   Reynolds; https://flic.kr/p/bkGzmb), #35 (sébastien bertru; https://flic.kr/p/ePUWLe), #36

461   (Mark Hodgson; https://flic.kr/p/eNZ2Ta), #37 (Susanne Nilsson; https://flic.kr/p/KHd9kZ),

462   #38 (sébastien bertru; https://flic.kr/p/84B5us), #39 (hedera.baltica;

463   https://flic.kr/p/G9QTtZ), #40 (Bernard Stam; https://flic.kr/p/dRYGZo), #41 (Smudge 9000;

464   https://flic.kr/p/zV4BHY), #42 (USFWS Endangered Species; https://flic.kr/p/8FgABc), #43

465   (Juan Emilio; https://flic.kr/p/nBU8Pn), #44 (Michele Lamberti; https://flic.kr/p/eWPGT9),

466   #45 (Bernard DUPONT; https://flic.kr/p/kwPAX3), #46 (Jason Crotty;

467   https://flic.kr/p/cfv8S5), #47 (Ron Kinight; https://flic.kr/p/nTru5f), #48 (Alastair Rae;

468   https://flic.kr/p/a2mZnM), #49 (Lip Kee; https://flic.kr/p/tFUR4u), #50 (Andrej Chudý;

469   https://flic.kr/p/4FxzSW), #51 (Francesco Veronesi; https://flic.kr/p/HmKL1U), #52 (Oona

470   Räisänen; https://flic.kr/p/qMQXuG), #54 (Michele Lamberti; https://flic.kr/p/eBu3YZ), #55

471   (Peter Trimming; https://flic.kr/p/bKYqJk), #56 (sébastien bertru; https://flic.kr/p/eQ7D8j),

472   #57 (Frank Vassen; https://flic.kr/p/9akQva), #58 (Ron Knight; https://flic.kr/p/diXcbm), #59

473   (Lip Kee; https://flic.kr/p/4mZKMQ), #60 (Mike Prince; https://flic.kr/p/8jvqN8), #61 (Jason

474   and Alison; https://flic.kr/p/8YiNML), #62 (Ferran Pestaña; https://flic.kr/p/8QCbQk), #63

475   (Jörg Hempel; https://flic.kr/p/7spWru), #64 (Derek Keats; https://flic.kr/p/pQn429), #65

476   (Ron Knight; https://flic.kr/p/diXchB), #66 (Frank Vassen; https://flic.kr/p/bVSw7h), #67

477   (Frank Vassen; https://flic.kr/p/s9ECnq), #68 (Frank Vassen; https://flic.kr/p/aUyu1z), #69

478   (Francesco Veronesi; https://flic.kr/p/ob6q3w), #70 (Ron Knight; https://flic.kr/p/diXePW),

479   #71 (Michele Lamberti; https://flic.kr/p/ecmCqj).

480

481   **Fig. 2.** HPLC chromatograms for (A) melanin marker (PTCA, PDCA, TTCA and 4-AHP)

482   standards and (B) feather samples from two species of birds included in the study as

483   examples.

484

485   **Fig. 3.** Mean reflectance spectra (± s.e.) of the specimens used in the study. The colors of

486   symbols represent the different color categories of the animals considered: black, grey,

487   dark brown, dark orange, light brown and light orange.

488

489   **Fig. 4.** Relationship between melanin-based color category in 59 species of birds and 12

490   species of mammals and two color expression measures: color slope (left axis, solid

491   symbols and continuous line) and brightness (right axis, open symbols and dashed line).

492   Color category refers to a scale based on the human perception of melanin-based color

493   variation, increasing with decreasing perceived darkness. Inserts are photographs

494   showing examples of these categories with details of color patches for some species

495   included in the study (from 1 to 6): *Fulica atra* (black), *Larus argentatus* (grey), *Mustela*

496   *erminea* (dark brown), *Coracias garrulus* (dark orange), *Gazella dorcas* (light brown) and

497   *Saxicola rubetra* (light orange). Complete photographs of these species are shown in Fig.

498   1. Slope refers to the slope of the regression between the amount of light reflectance and

499   wavelength in the range 400-700 nm, and brightness refers to the summed reflectance in

500   that range. The lines are the regression lines.

501

502   **Fig. 5.** Relationship between color phenotype (expressed as the slope of the amount of

503   light reflectance regressed against wavelength) and the scores of a partial least-squares

504   regression (PLSR) component related to the melanin composition of feathers and hairs.

505   The names of significant predictors below the PLSR component indicate which side of the

506   axis increased with increasing values. The line is the regression line. The point on the top

507   right of the figure is not an outlier, as indicated by a Cook's distance (0.51) smaller than 2

508   and a leverage (0.04) smaller than 2p/n (0.05; p is the number of parameters in the model
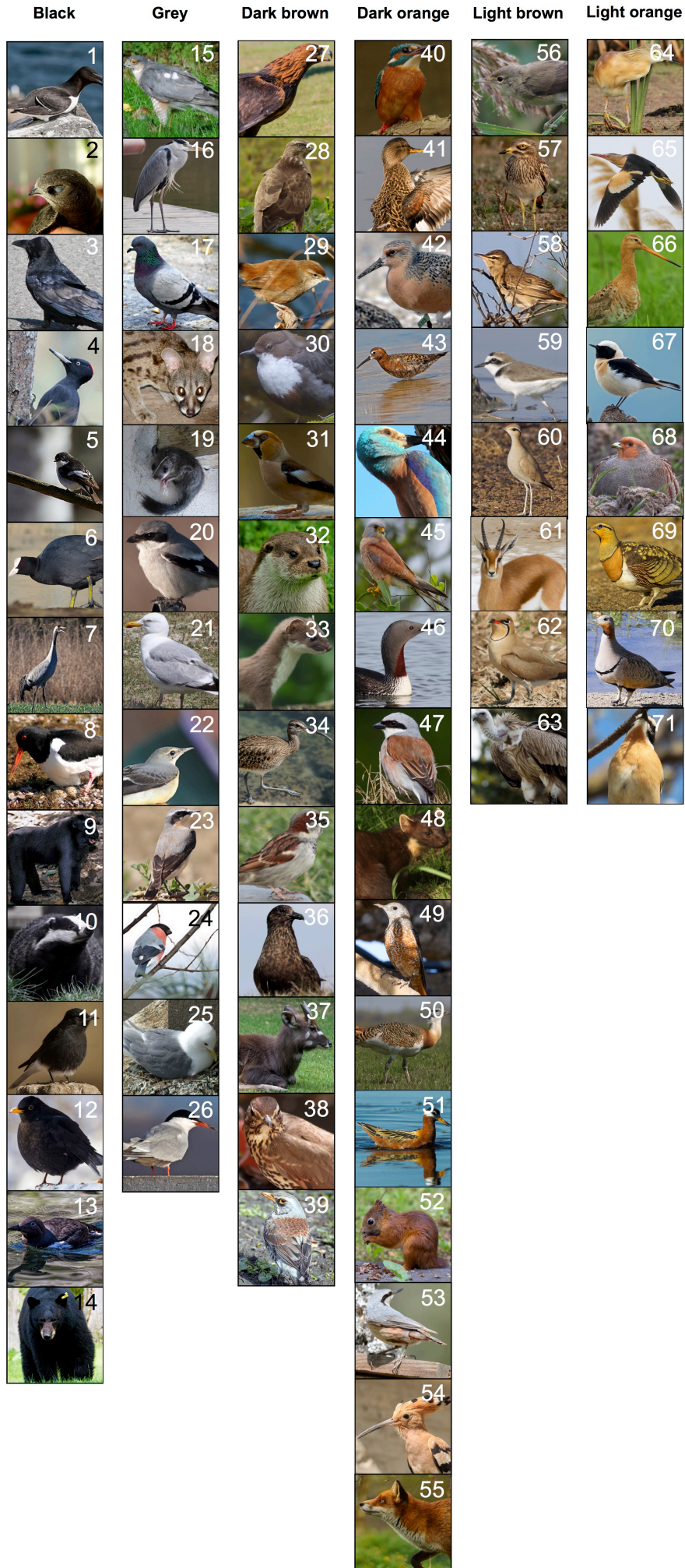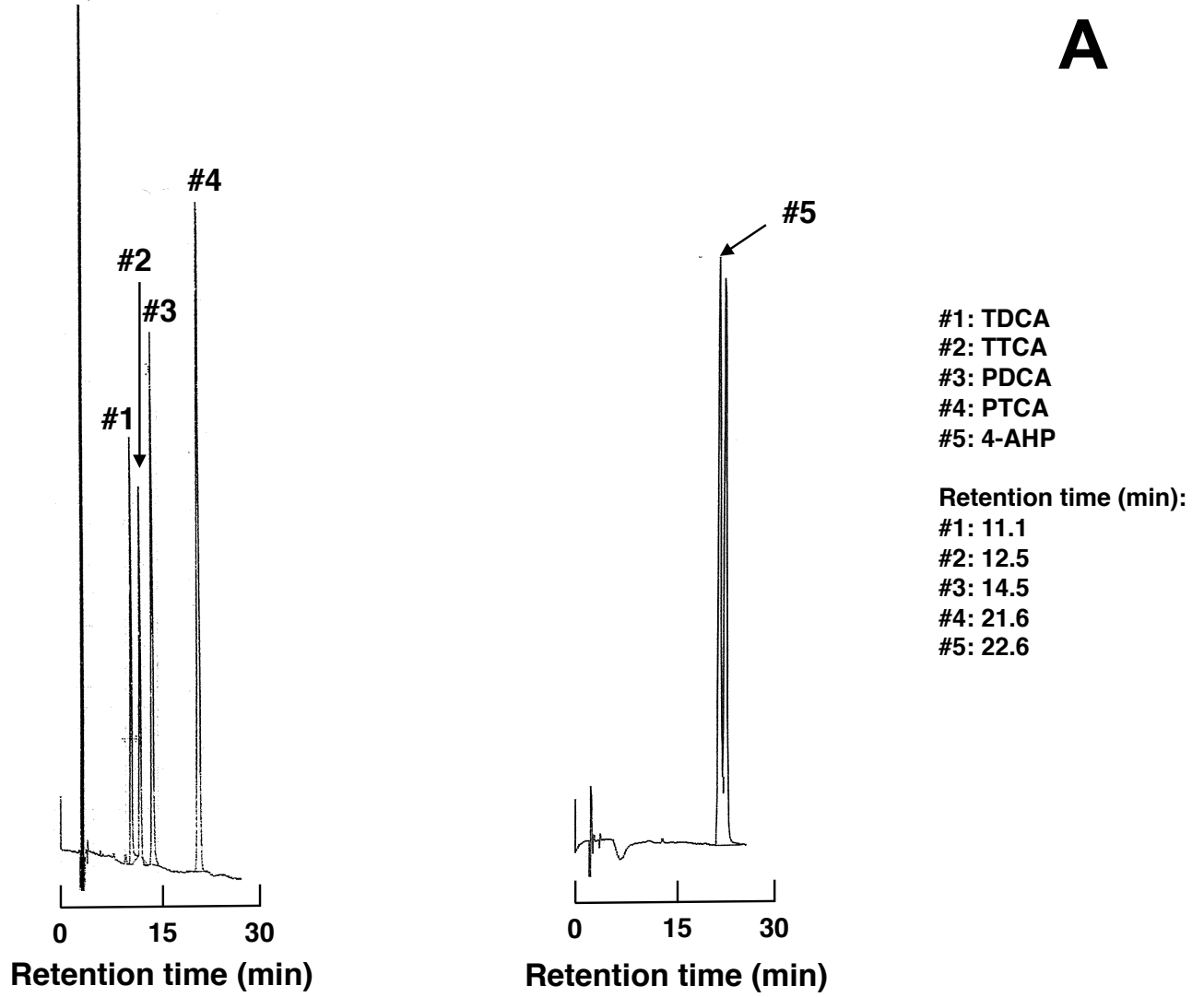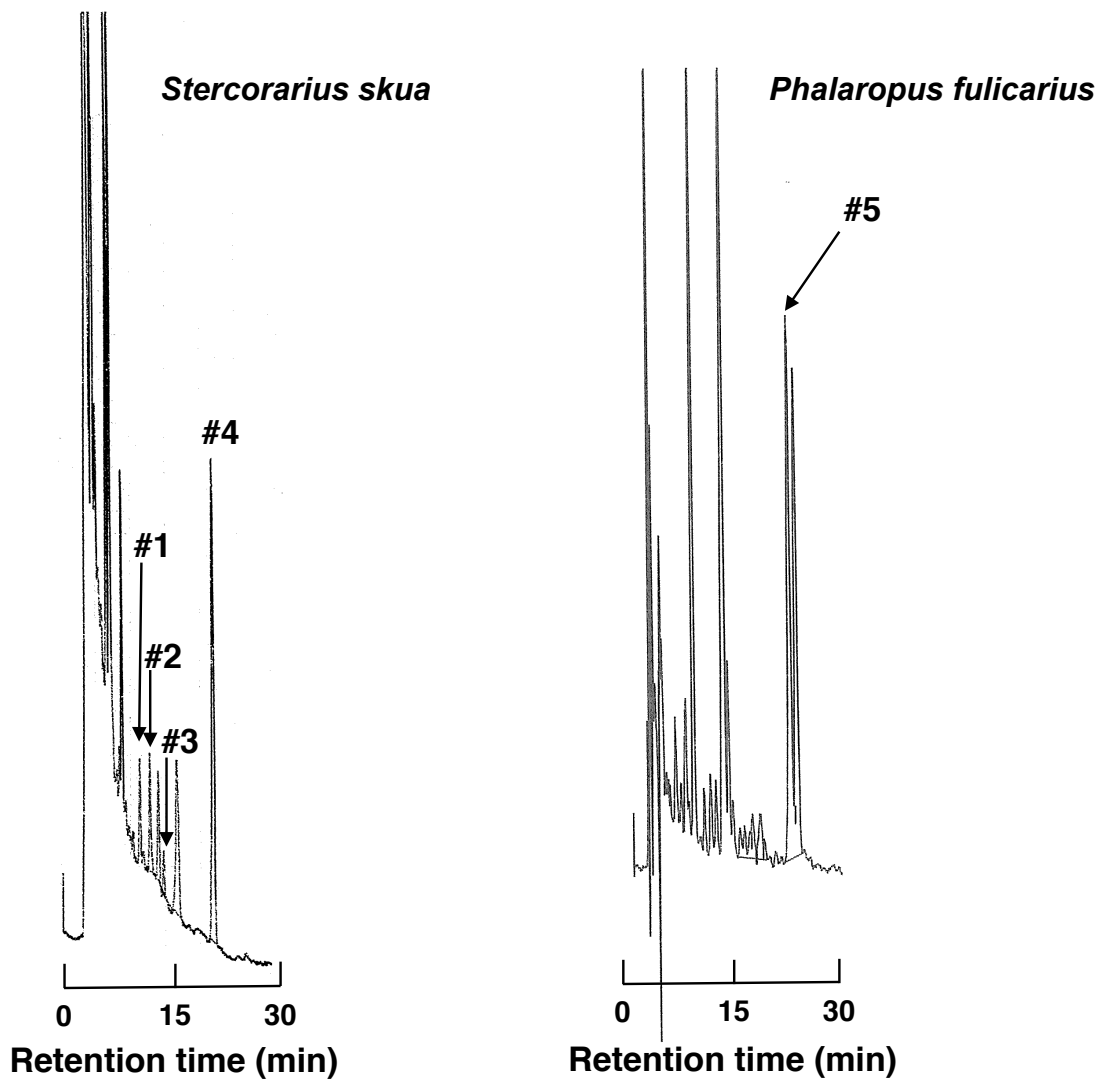
509   and n is the sample size)[34].

Black   Grey   Dark brown   Dark orange   Light brown   Light orange

Figure 1

A

#1: TDCA
#2: TTCA
#3: PDCA
#4: PTCA
#5: 4-AHP

Retention time (min):
#1: 11.1
#2: 12.5
#3: 14.5
#4: 21.6
#5: 22.6

Retention time (min)

Retention time (min)

B
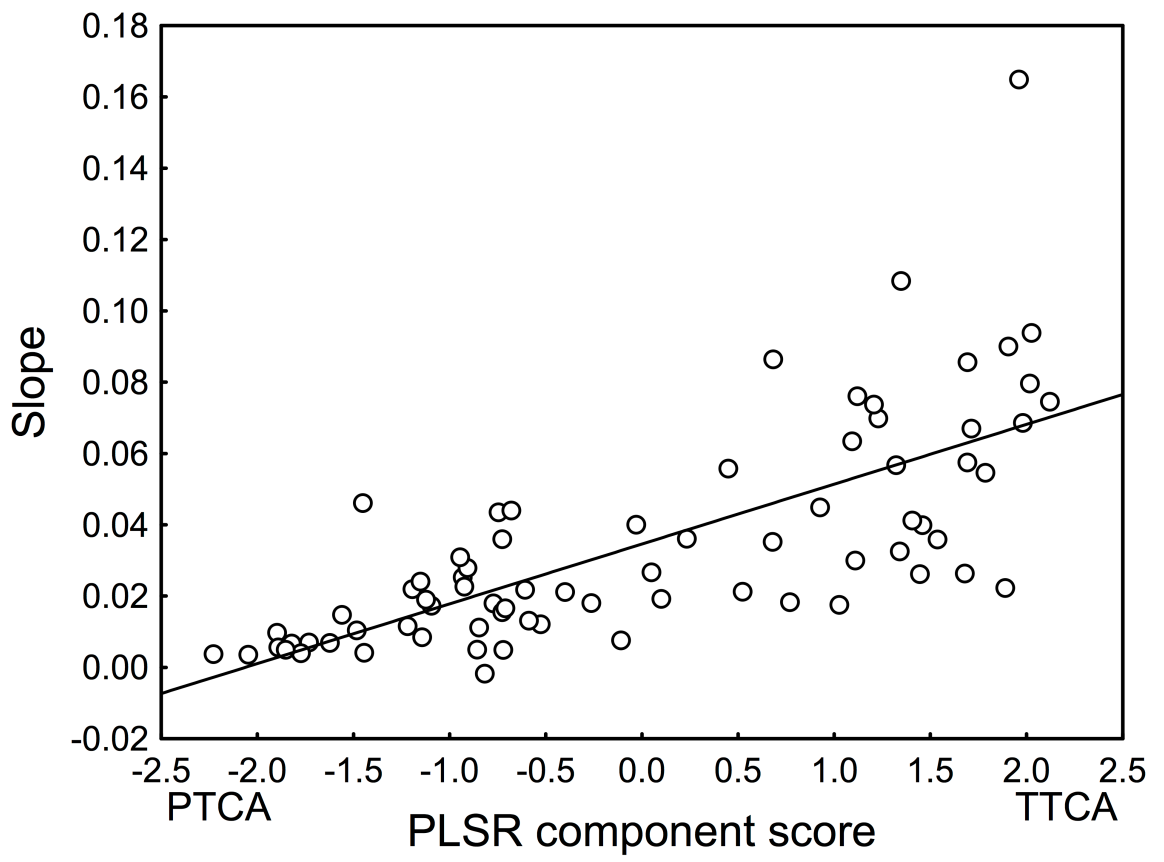
Stercorarius skua

Phalaropus fulicarius

Retention time (min)

Retention time (min)
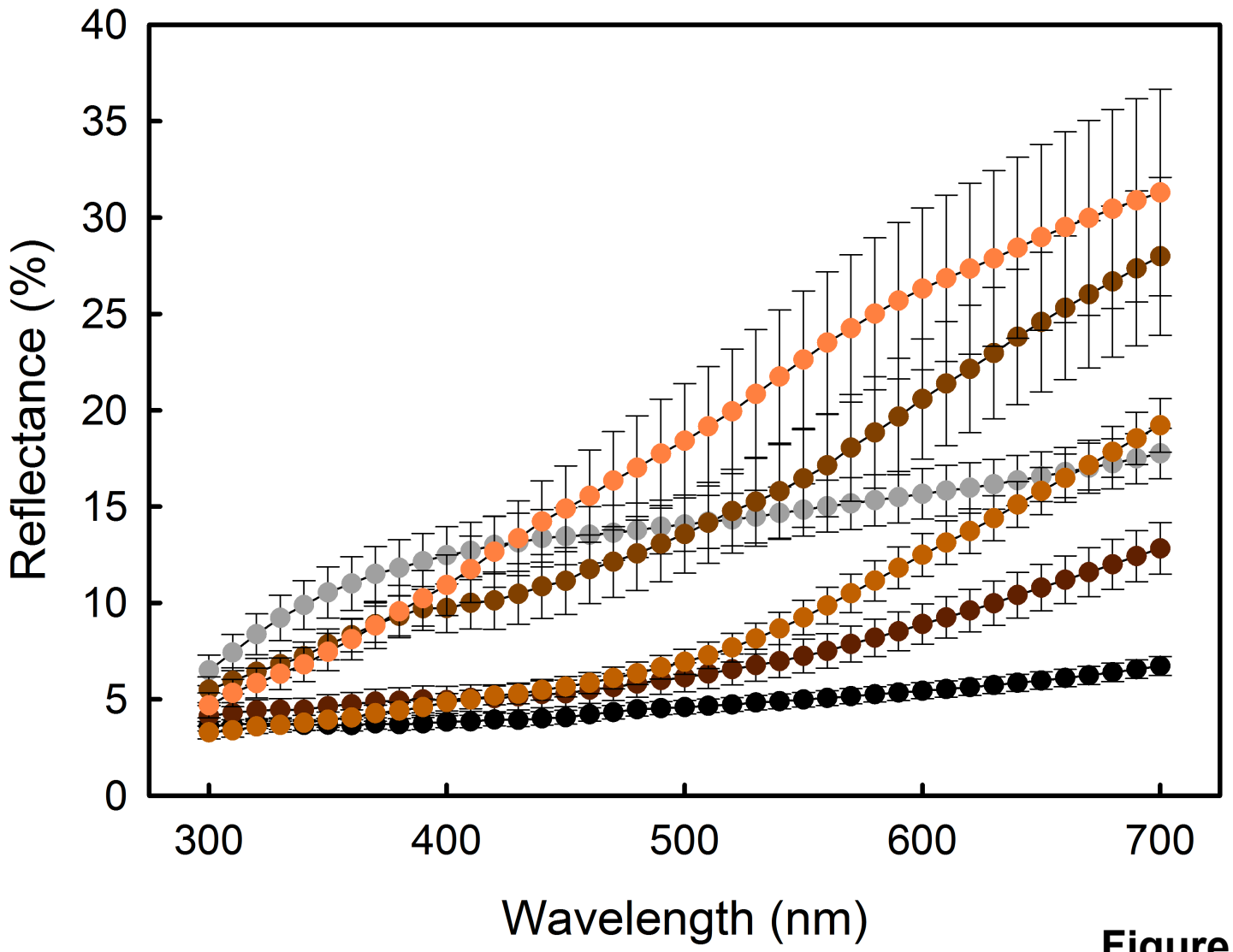
Figure 2

Figure 3

Figure 4

Figure 5